JACS
JOURNAL OF THE AMERICAN CHEMICAL SOCIETY
Article
pubs.acs.org/JACS

Water of Hydration Dynamics in Minerals Gypsum and Bassanite: Ultrafast 2D IR Spectroscopy of Rocks

Chang Yan, Jun Nishida, Rongfeng Yuan, and Michael D. Fayer*

Department of Chemistry, Stanford University, Stanford, California 94305, United States

Supporting Information

ABSTRACT: Water of hydration plays an important role in minerals, determining their crystal structures and physical properties. Here ultrafast nonlinear infrared (IR) techniques, two-dimensional infrared (2D IR) and polarization selective pump−probe (PSPP) spectroscopies, were used to measure the dynamics and disorder of water of hydration in two minerals, gypsum ($CaSO_4{\cdot}2H_2O$) and bassanite ($CaSO_4{\cdot}0.5H_2O$). 2D IR spectra revealed that water arrangement in freshly precipitated gypsum contained a small amount of inhomogeneity. Following annealing at 348 K, water molecules became highly ordered; the 2D IR spectrum became homogeneously broadened (motional narrowed). PSPP measurements observed only inertial orientational relaxation. In contrast, water in bassanite's tubular channels is dynamically disordered. 2D IR spectra showed a significant amount of inhomogeneous broadening caused by a range of water configurations. At 298 K, water dynamics cause spectral diffusion that sampled a portion of the inhomogeneous line width on the time scale of ∼30 ps, while the rest of inhomogeneity is static on the time scale of the measurements. At higher temperature, the dynamics become faster. Spectral diffusion accelerates, and a portion of the lower temperature spectral diffusion became motionally narrowed. At sufficiently high temperature, all of the dynamics that produced spectral diffusion at lower temperatures became motionally narrowed, and only homogeneous broadening and static inhomogeneity were observed. Water angular motions in bassanite exhibit temperature-dependent diffusive orientational relaxation in a restricted cone of angles. The experiments were made possible by eliminating the vast amount of scattered light produced by the granulated powder samples using phase cycling methods.

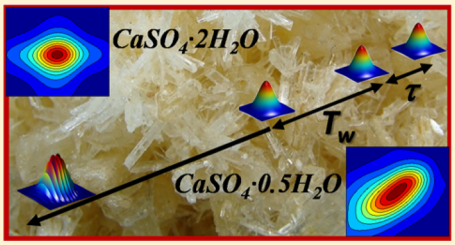

1. INTRODUCTION

In nature, water exists in a variety of forms other than bulk liquid water. Water is often found to be physically adsorbed in small pores of rocks and zeolites or occupying the volume of confined interstitial sites in the Earth's sediment. Hydrous minerals, such as gypsum, opal, borax, chalcancite, epsomite, and smectite, etc., are common. The water of hydration in these natural crystals plays important roles in co-constituting the structural frameworks with mineral ions.

Water of hydration molecules in minerals, in general, do not form the extended hydrogen-bonding network found in bulk liquid water. Instead, depending on the specific chemical structure of a mineral, water molecules form different types of hydrogen bonds with anions or coordinate with metal cations. The interactions between water molecules and minerals have a large impact on the physical and chemical properties of both. For example, sodium sulfate has a low melting point of ∼32.4 °C in its decahydrate form (Glauber's salt), and has been explored as an effective material for phase change energy storage.[1] The water of hydration's low vapor pressure also allows water to exist in this form even under extreme conditions such as the surface of Mars.[2]

The bulk liquid water is well-known to undergo ultrafast structural dynamics. Dynamics, such as molecular reorientation[3] and hydrogen-bonding network rearrangement,[4] take place on the time scales of femtoseconds (fs) and picoseconds (ps). Although water molecules embedded in solid frameworks are structurally confined, they can still undergo fast dynamics. The enthalpy of formation for hydrogen bonds between water molecules and other species is usually only a few kcals per mole. The relatively weak interactions make it possible for water molecules to sample different structural configurations under ambient conditions, especially when water sites are located inside the cavities or tubes formed by mineral ions.[5] Viewing the water of hydration structure in minerals as static provides an incomplete perspective.

The time-average structure of water of hydration in mineral crystals has been extensively investigated by techniques including X-ray diffraction,[6] neutron scattering,[7] nuclear magnetic resonance (NMR),[8] linear infrared (IR) absorption spectroscopy,[9] and dielectric spectroscopy.[10] Line shape analysis of one-dimensional frequency-domain spectra can provide some time-domain information on water dynamics. Water motion on picosecond time scales has been studied by line shape analysis of the results from dielectric spectroscopy,[11] NMR spectroscopy,[12] and quasi-elastic neutron scattering experiments.[13] However, such analysis depends on the specific models chosen to describe the broadening mechanism of spectral lines.[3] In many circumstances in which spectral lines

Received: May 31, 2016
Published: July 7, 2016

DOI: 10.1021/jacs.6b05589
J. Am. Chem. Soc. 2016, 138, 9694−9703

are complicated by various inhomogeneous broadening mechanisms, line shape analysis only provides a rough estimation of time scales, and the interpretation of these results needs to be aided by other methods such as molecular dynamics simulations.[14,15] Molecular dynamics simulations have provided insights into water dynamics in minerals.[16]

Ultrafast nonlinear IR spectroscopies are useful methods for directly measuring water dynamics in the time domain.[3,17−20] The observables of these experiments can be conveniently compared to molecular dynamics simulations on ultrafast time scales.[19,21,22] IR polarization selective pump−probe (PSPP) spectroscopy monitors the angular motion of water molecules by measuring the time-dependent anisotropy decay. Two-dimensional IR (2D IR) spectroscopy measures the evolution of vibrational frequencies with time (spectral diffusion). The vibrational spectrum of the hydroxyl stretch mode of water is highly sensitive to water molecules' chemical environments. A range of environments gives rise to an inhomogeneously broadened hydroxyl stretch absorption spectrum. At time $t = 0$, a given water hydroxyl will have a specific frequency within the inhomogeneously broadened absorption line. If the structural environment evolves in time, the hydroxyl stretch will undergo spectral diffusion, that is, sample different frequencies within the inhomogeneously broadened spectrum. Spectral diffusion is caused by the structural evolution of the system. Therefore, 2D IR spectroscopy provides direct measurements of the time dependence of a system's structural dynamics.

2D IR and PSPP techniques have been used extensively for studying water dynamics in a wide variety of liquid systems, e.g., bulk water, reverse micelles, and water in room-temperature ionic liquid systems. All such systems have high optical quality, producing little scattered light that generally interferes with the measurements. However, the mineral samples studied here are granular solid powders that produce an enormous amount of scattered light and cannot be studied using the IR nonlinear experimental methodology that works well for optically clear liquid samples. Using a recently developed phase cycling technique for removing scattering from the nonlinear IR signal,[23] we were able to conduct 2D IR and PSPP experiments to study the water of hydration in two minerals, gypsum ($CaSO_4{\cdot}2H_2O$) and bassanite ($CaSO_4{\cdot}0.5H_2O$).

Gypsum is one of the most commonly mined hydrous minerals. It has routine uses in fertilizers, constituents of plasters, and chalks. Its lattice can be viewed as a pattern of alternating water layers and calcium sulfate layers (see Figure 1A).[24] All water molecules are identical in the lattice, but each water molecule forms two nonidentical hydrogen bonds with two different sulfate ions (blue dashed lines in Figure 1A). At an elevated temperature, gypsum can be partially dehydrated to form a different mineral, bassanite, which is also found in nature. Removal of the water produces a change in the lattice structure from the planar structure of gypsum to tubular channels in the lattice of bassanite (dashed black circle in Figure 1B).[25] Isolated water molecules reside in these channels and form weak hydrogen bonds with sulfate ions. The water molecules have large thermal displacements as reported from diffraction experiments.[25,26] Previous inelastic neutron scattering experiments performed at low temperatures (3 and 150 K) also suggest that water molecules are dynamically disordered.[5,27]

Here 2D IR spectroscopy revealed that the water arrangement in solution-derived fresh gypsum was slightly disordered. After annealing at 348 K, almost all of the disorder was removed, and the 2D IR spectrum is overwhelmingly dominated by homogeneous broadening. The only angular motion of water in annealed gypsum reported by PSPP spectroscopy is ultrafast inertial motion with a half angle <15°. In contrast, the 2D IR spectrum of bassanite contains a significant amount of inhomogeneous broadening. Part of the inhomogeneous water configurations can be dynamically sampled with a spectral diffusion rate on the time scale of tens of picoseconds at room temperature, while the rest of inhomogeneity is static within the experimental time window, which is limited by the vibrational lifetime of the hydroxyl stretch. As the temperature is increased, the spectral diffusion becomes faster and more of the inhomogeneity is motionally narrowed, becoming part of the homogeneous component of the spectrum. At sufficiently high temperature, 348 K, only homogeneous broadening and the static component of the inhomogeneous broadening were observed. PSPP measurements of orientational relaxation show that water molecules undergo wobbling motion in a diffusive cone with a restricted half angle of ∼25°. The orientational dynamics are also temperature-dependent.

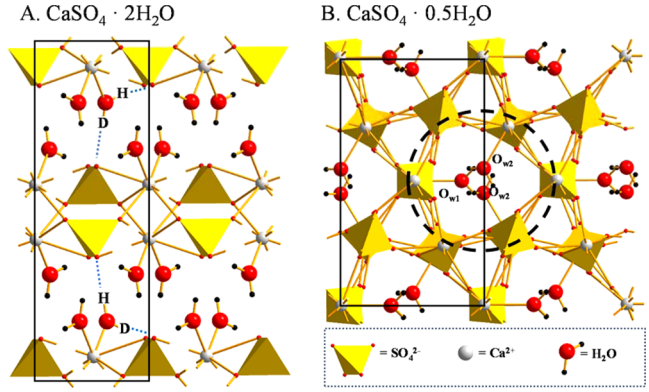

Figure 1. Crystal structure of gypsum (A) and bassanite (B) viewed along the [001] vector. The black solid frame identifies the (001) face of each unit cell. In panel A, each water molecule is identical in a gypsum unit cell and forms two nonidentical hydrogen bonds (blue dashed line) with two sulfate ions. Water oxygens and sulfate oxygens coordinate around calcium ions (yellow solid lines). In panel B, isolated water molecules reside in channels (black dashed circle) formed by sulfate ions. Two types of water sites exist (O_{w1} and O_{w2}). The diameter of the channel is ∼5.5 Å.

2. EXPERIMENTAL METHODS

2.1. Sample Preparation and Characterization. Fresh gypsum crystals were precipitated by mixing a $CaCl_2$ aqueous solution and a Na_2SO_4 aqueous solution. In the solution, 1% of all the water molecules were HOD molecules, with the rest being H_2O. Studying the OD stretch avoids coherent and incoherent vibrational energy transfer between the symmetric and asymmetric stretch modes of H_2O or D_2O. In addition, looking at the OD stretch of dilute HOD eliminates the possibility of intermolecular vibrational excitation transfer.[17] To anneal the gypsum, the precipitated crystallites were first ground and mixed with Nujol oil. Then the mixture was kept in a sealed sample cell and held at 348 K for 24 h. No dehydration was observed in the annealing process by comparing the Fourier transform infrared (FT-IR) spectra before and after holding the sample at the elevated temperature.

Bassanite powder samples were prepared by heating gypsum powder under a constant flow of air containing deuterated water vapor at ∼388 K. The deuterium content in bassanite was controlled by the deuterium content of the water vapor. The water vapor consisted of

DOI: 10.1021/jacs.6b05589
J. Am. Chem. Soc. 2016, 138, 9694−9703

82.8% H_2O, 16.4% HOD, and 0.8% D_2O. In bassanite, water molecules are separated by ~5 Å, and therefore intermolecular vibrational excitation transfer is largely absent. The deuterium ratio here was chosen to maximize the HOD content for 2D IR experiments while keeping the D_2O peaks from complicating spectral analysis.

FT-IR spectra of Nujol oil mixture containing gypsum or bassanite were measured with a Thermo Scientific Nicolet 6700 FT-IR spectrometer with 0.5 cm^{-1} resolution. The spectrum of Nujol oil was subtracted from each sample spectrum to yield the background-free data. Structures of synthesized gypsum and bassanite were also characterized by X-ray powder diffraction and thermal gravity analysis (see Supporting Information). Gypsum and bassanite powders were stored in a drybox constantly purged with a positive pressure of dry air. The deuterium content was checked by FT-IR spectra, and the content was not changed even after months of storage. For both minerals, crystal particles were ground to sizes less than a few microns before time-resolved measurement to ensure that a large number of small crystallites were within the laser spot and were randomly oriented.

2.2. 2D IR and PSPP Experiments. The 2D IR and PSPP experiments were performed using the same optical setup with pump−probe beam geometry. The details of 2D IR experiments have been documented previously.[28,29] A mid-IR optical parametric amplifier pumped by a Ti:sapphire regenerative amplifier produced ~170 fs pulses centered at the frequency of interest (gypsum or bassanite absorption center), with ~10 μJ pulse energy. The mid-IR pulses were then split into a weak probe pulse and a strong pump pulse. The pump pulse passed through an acousto-optic mid-IR Fourier-domain pulse shaper to be further split into pulses 1 and 2, which were collinear but separated by a controllable time delay, τ. Pulses 1 and 2 were focused on the sample, and the probe pulse (pulse 3) arrived after a waiting time T_w which was controlled by a mechanical delay line.

The first two pulses labeled the initial vibrational frequencies within the inhomogeneous absorption spectrum. These initial frequencies give the ω_τ horizontal axis of the 2D IR spectrum. After a waiting time, T_w, during which the sample structure can evolve, pulse 3 stimulates the emission of the vibrational echo pulse. Pulse 3 and the vibrational echo pulse propagate collinearly. Pulse 3 serves as the local oscillator (LO) to heterodyne-detect the echo. The combined LO/echo pulse is dispersed by a monochromator acting as a spectrograph and detected with a 32 element MCT array. The dispersed echo pulse gives the frequencies after T_w, the ω_m vertical axis of the 2D spectrum. At each T_w, τ was scanned to move the echo in time relative to pulse 3. This process generates an interferogram at each ω_m frequency. The interferograms were numerically Fourier transformed to give the ω_τ axis in the 2D spectrum.

During the period T_w, structural evolutions of water and surrounding ions cause the vibrational frequency of OD stretch to evolve and therefore the shape of 2D IR spectra to change. The dynamical information of interest is contained in the T_w-dependent frequency-frequency correlation function (FFCF). The FFCF describes the probability that a vibrational oscillator will have the same frequency at time t as it did at $t = 0$, averaged over all initial frequencies in the inhomogeneous line shape. The FFCF is quantified via a 2D line shape analysis known as the center line slope (CLS) method.[30,31] The CLS is equivalent to the T_w-dependent portion of the normalized FFCF. To calculate the CLS from the 2D spectrum at a given T_w, a series of slices parallel to the ω_m axis through the 2D spectrum in the region around the spectrum center are obtained. Each slice is a 1D spectrum. The center line consists of the set of points that are located at the peaks of these 1D spectra obtained from the cuts, and the CLS is the slope of this line. In general, as T_w is increased, the shape of the 2D spectrum changes, and the CLS changes. A plot of the CLS vs T_w is the normalized T_w-dependent portion of the FFCF. Combining the CLS curve with the absorption spectrum provides the full FFCF including the homogeneous contribution to the absorption spectrum.

The FFCF can be modeled as a sum of exponentials:

$$C(t) = \langle \delta\omega(t)\delta\omega(0)\rangle = \sum_i \Delta_i^2 \exp(-t/\tau_i) \quad (1)$$

where $\delta\omega(t) = \omega(t) - \langle\omega\rangle$ is the instantaneous frequency fluctuation, Δ_i is the frequency fluctuation line width of the i^{th} inhomogeneous contribution to the total line width, and τ_i is the associated spectral diffusion time constant. Δ_i is the standard deviation of the Gaussian line profile associated with the i^{th} inhomogeneous broadening term. In the case where τ_i is too slow to measure during the experimentally accessible range of T_ws, the inhomogeneous component will be described by a constant term in the FFCF. In the case of $\Delta\tau < 1$ (Δ in the unit of rad/ps and τ in the unit of ps), this component of the FFCF is motionally narrowed and contributes to the homogeneous line width. For the motionally narrowed term, Δ and τ cannot be determined separately. The deviation from unity of the CLS at $T_w = 0$ ps determines the homogeneous broadening component's relative amplitude in the normalized FFCF. In the total absorption line shape, the homogeneous broadening term has a Lorentzian line shape and a pure dephasing line width $\Gamma^* = \Delta^2\tau = 1/(\pi T_2^*)$, where T_2^* is the pure dephasing time. The total homogeneous dephasing time T_2 is given by $\frac{1}{T_2} = \frac{1}{T_2^*} + \frac{1}{2T_1} + \frac{1}{3T_{or}}$, where T_1 is the vibrational lifetime and T_{or} is the orientational relaxation time. Here T_1 and T_{or} are sufficiently slow compared to T_2^* that $T_2^* \approx T_2$.

The line width of each FFCF component, Γ and Δ_i, in the unit of cm^{-1} is obtained from a simultaneous fit to the CLS decay measured by 2D IR and the total linear absorption line shape measured by FT-IR.[30,31] The total inhomogeneous broadening line width (standard deviation) Δ_{inh} is given by $\Delta_{inh} = (\sum_i \Delta_i^2)^{1/2}$. It is important to note that the CLS decay is an experimental observable that is independent of a specific dynamic model. The exponential time constants characterize the time scale of the observed dynamics rather than being strictly associated with a single structural event.

The PSPP experiments were performed to examine the reorientation dynamics of the water molecules. In PSPP experiments, the pump pulse is a single pulse, but the pulse shaper was still used for phase cycling. The polarization of pump pulse was set to 45° relative to the probe pulse. The probe transmission's intensity with polarizations parallel and perpendicular to the pump polarization, $S_\parallel(t)$ and $S_\perp(t)$, respectively, were resolved by a polarizer mounted in a motorized rotation stage after sample, and t is the time delay between the pump and the probe pulses. The decay of $S_\parallel(t)$ and $S_\perp(t)$ versus t are

$$S_\parallel(t) = P(t)[1 + 0.8C_2(t)] \quad (2)$$

$$S_\perp(t) = P(t)[1 - 0.4C_2(t)] \quad (3)$$

where $P(t)$ is the population relaxation and $C_2(t)$ is the second Legendre polynomial orientational relaxation correlation function of the vector pointing along the OD bond in a HOD molecule. From $S_\parallel(t)$ and $S_\perp(t)$, the population relaxation, $P(t)$, and the anisotropy relaxation, $r(t)$, can be obtained as

$$P(t) = S_\parallel(t) + 2S_\perp(t) \quad (4)$$

$$r(t) = \frac{S_\parallel(t) - S_\perp(t)}{S_\parallel(t) + 2S_\perp(t)} = 0.4C_2(t) \quad (5)$$

Then, $r(t)$ is the orientational relaxation correlation function multiplied by 0.4.

2.3. Removing the Scattering Light with Phase Cycling. The powder samples were blended with Nujol oil and sealed in a sandwich sample cell so that the scattered light was substantially reduced via refractive index matching. However, the remaining scattered light is still so large that under normal experimental conditions, it would not be possible to do either the 2D IR or PSPP experiments. All 2D IR experiments were performed under $\langle XXYY\rangle$ polarization scheme where pulses 1 and 2 (YY) have perpendicular polarization relative to pulse 3 and echo pulse (XX). The combined LO/echo pulse was passed through a resolving polarizer set to X polarization to filter out a substantial amount of the scattered light from pulses 1 and 2. The remaining, still significant, amount of scattering from all pulses was

DOI: 10.1021/jacs.6b05589
J. Am. Chem. Soc. 2016, 138, 9694−9703

removed by recording the signal with an 8-shot phase cycling scheme:[23]

$$\{[(0, 0, \mathrm{OFF}) - (0, 0, \mathrm{ON})] - [(0, \pi, \mathrm{OFF}) - (0, \pi, \mathrm{ON})]\} + \{[(\pi, \pi, \mathrm{OFF}) - (\pi, \pi, \mathrm{ON})] - [(\pi, 0, \mathrm{OFF}) - (\pi, 0, \mathrm{ON})]\} \quad (6)$$

where (φ1,φ2,chop) is the LO/echo heterodyne signal intensity on the detector with the phases of pulses 1 and 2 set to $\varphi_i = 0$ or π, and the chopper on the probe path set to OFF (pulse 3 block) or ON. The phases of pulses 1 and 2 were controlled by the pulse shaper.

For the PSPP experiments, we detected the probe transmission's intensity rather than extracting its phase information. Therefore, a 4-shot phase cycling scheme was applied to remove t-dependent scattering terms which interfere with the data. The scattering terms independent of t resulted in a time independent offset and were removed by baseline subtraction. The data recorded with the 4-shot phase cycling scheme is expressed as follows: $[(0) - (\mathrm{OFF})] + [(\pi) - (\mathrm{OFF})]$, where (0) and ($\pi$) correspond to the pump pulse's phase set to 0 and π by the pulse shaper, and (OFF) corresponds to the pump pulse turned off by the pulse shaper.

3. RESULTS AND DISCUSSION

3.1. Gypsum. Figure 2 shows the FT-IR spectrum of freshly prepared solution-derived gypsum (black curve). In gypsum,

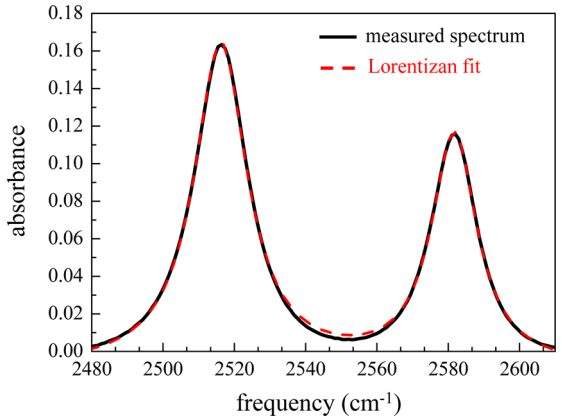

Figure 2. FT-IR spectrum (solid black curve) of the OD stretch of HOD in gypsum in which 1% of the water molecules are HOD. The red dashed curve is the fit to two Lorentzians.

the OD bonds of HOD molecules form two different types of hydrogen bonds with sulfate ions.[32] As a result, two OD stretch peaks are observed at 2514 and 2583 cm^{-1}.[32] The lower frequency OD mode corresponds to a hydrogen bond where the O−O distance (water oxygen to sulfate oxygen) is 2.81 Å, whereas the higher frequency mode corresponds to a different hydrogen bond with an O−O distance of 2.88 Å.[24] The correlation between the hydrogen bond O−O distance and the hydroxyl stretch frequency at the peak center in minerals has been summarized by the following equation:

$$\nu = \nu_0 - 3.04 \times 10^{11} e^{-d_{O-O}/0.1321} \quad (7)$$

where ν_0 is an adjustable frequency parameter in the unit of cm^{-1} dependent on the specific system, and d_{O-O} is the O−O distance in the hydrogen bond in the unit of Å.[33]

Given that ν = 2514 cm^{-1} and d_{O-O} = 2.81 Å, we can calculate ν_0 = 2690 cm^{-1} in the sulfate-water system here. In turn, if d_{O-O} = 2.88 Å, we have ν = 2586 cm^{-1}, which agrees well with the measured peak center at 2583 cm^{-1}. The effectiveness of calibration using the band at 2514 cm^{-1} stems from the fact that the interactions between water, Ca^{2+} and SO_4^{2-} in gypsum, or bassanite are similar in nature and only differ in strength. Water oxygens coordinate with Ca^{2+} cations, and water hydrogens form hydrogen bonds with SO_4^{2-} anions.

The two types of hydrogen bonds exist in a population ratio of 1:1, and the difference in the absorbance of the two peaks is a result of different transition dipoles. A stronger hydrogen bond results in a larger transition dipole and a larger absorbance. Shorter hydrogen bonds are stronger, which is consistent with the lower frequency peak having a larger absorbance.

The spectrum (black curve) in Figure 2 was fit exceedingly well with the sum of two Lorentzian bands (red curve). A Lorentzian shape is indicative of a homogeneously broadened absorption. However, it is not possible to determine from the spectrum whether there is a Gaussian contribution reflecting inhomogeneous broadening but with the width of the Gaussian too narrow to be detected by a deviation from the apparent Lorentzian line shape. The linear absorption spectrum indicates that both bands are substantially homogeneously broadened. The linear absorption spectrum of annealed gypsum is basically the same as the fresh gypsum's spectrum shown in Figure 2.

The vibrational population relaxation lifetimes of the OD stretch in the two hydrogen-bonding configurations are 5.70 ± 0.05 ps for 2514 cm^{-1} and 6.94 ± 0.05 ps for 2583 cm^{-1}. The shorter lifetime associated with the lower frequency peak is likely caused by the stronger hydrogen bonding to the sulfate, which enhances the flow of vibrational energy out of the excited OD stretch into other vibrational modes of the system. For comparison, the OD stretch of HOD in H_2O is 1.8 ps.[34]

The relatively long lifetime enables the anisotropy decay of OD stretch mode of the HOD molecule to be measured to ∼15 ps. The time-dependent anisotropy data (circles) of fresh and annealed gypsum are shown in Figure 3. In all of the curves, anisotropy values fluctuate within approximately ±0.01 around the initial anisotropy values at t = 0.5 ps. The solid lines are horizontal fits to the data. The results indicate the lack of diffusive reorientation dynamics during the time period of measurement. The fact that there is no discernible slope to any of the data sets means any slow diffusive orientational relaxation would have a time constant longer than ∼1 ns. The deviation from 0.4 at t = 0 indicates that there is ultrafast motion (<100 fs) that samples a restricted cone of angles.[35] The OD bond vector samples a limited range of angles, but does not randomize its orientation. This type of ultrafast motion is generally taken to be inertial rather than diffusive.[35] The larger the deviation from 0.4 when the data are extrapolated to t = 0, the larger the cone angle.[35] Before annealing, the half angle for the OD bond associated with the weaker hydrogen-bonding configuration (2583 cm^{-1}, Figure 3B) is calculated to be 26°, clearly larger than the 16° half angle of the OD bonds with stronger hydrogen bonds (2514 cm^{-1}, Figure 3A). After annealing, both half angles decrease to smaller values: 14° for 2514 cm^{-1} and 11° for 2583 cm^{-1}.

The fact that annealing changes the cone angles shows that on average the lattice has reconfigured in a manner that is more restrictive in terms of the angular motions of the water of hydration. In terms of the harmonic cone model for restricted angular motion,[36] the reduction of the cone widths indicates that the potential has become steeper. The change in the lattice with annealing results in the hydroxyls experiencing a more restrictive (steeper) angular potential. It is interesting that annealing influenced the configuration that gives rise to the

DOI: 10.1021/jacs.6b05589
J. Am. Chem. Soc. 2016, 138, 9694−9703

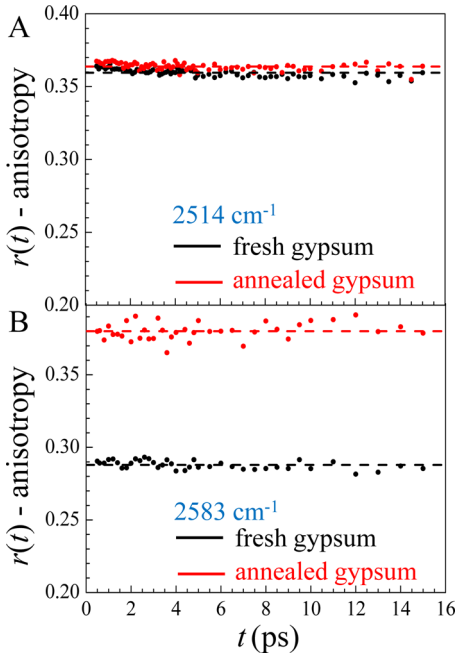

Figure 3. (A) Anisotropy data measured at 2514 cm^{-1} for fresh (black points) and annealed (red points) gypsum samples. The dashed lines are horizontal fits to the data. (B) Anisotropy data measured at 2583 cm^{-1} for fresh (black points) and annealed (red points) gypsum samples. The dashed lines are horizontal fits to the data. None of the data are decaying, showing that within the time window of the measurement, there is no orientational motion other than ultrafast inertial motions.

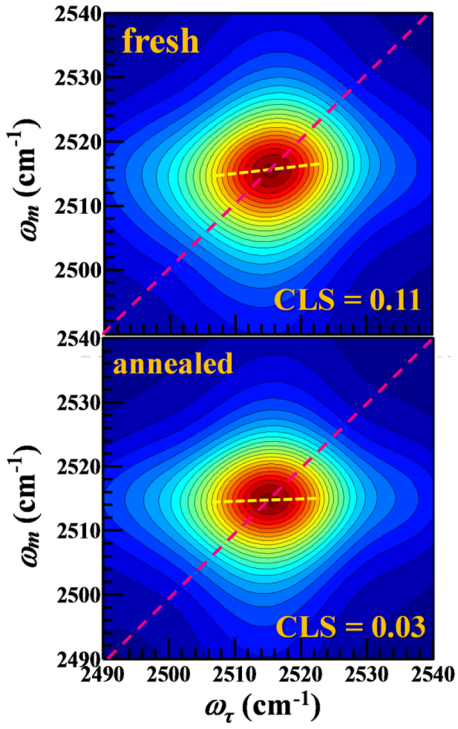

Figure 4. 2D IR spectra of fresh solution-derived gypsum (top panel) and annealed gypsum (bottom panel). The spectra are for the band at 2514 cm^{-1} and were taken at T_w = 0.5 ps. The slope of yellow dashed line is the center line slope. The dashed red line is the diagonal.

weaker hydrogen bond considerably more than to the stronger hydrogen bonded hydroxyl. Annealing does not affect the two types of hydrogen-bonding sites equally.

To gain additional information on the water dynamics in gypsum, 2D IR experiments were performed on both OD stretch bands in Figure 2. Figure 4 displays 2D IR spectra of fresh (top panel) and annealed (bottom panel) gypsum taken at T_w = 0.5 ps on the 0−1 transition of the band at 2514 cm^{-1}. The dashed red line is the diagonal. For a system for which the absorption spectrum is dominated by inhomogeneous broadening, the 2D spectrum will show extensive elongation along the diagonal at short T_w. There is no obvious elongation along the diagonal in Figure 4. The star-like shape of both 2D spectra implies that the lines are homogeneously broadened (Lorentzian absorption line shape) or close to homogeneously broadened with at most a small inhomogeneous Gaussian contribution. The 2D line shape is consistent with the Lorentzian line shape of linear IR absorption spectrum. The yellow dashed lines in Figure 4 are the center lines. For the fresh sample, the CLS is 0.11. The value's substantial deviation from 1 at T_w = 0 ps suggests that the water molecules in gypsum are highly ordered with almost identical chemical environment, but the nonzero CLS demonstrates that there is some degree of inhomogeneous broadening. The line broadening is dominated by homogeneous dephasing (motional narrowing), most likely caused by coupling of the hydroxyl-sulfate configurations to lattice phonons, which induce ultrafast structural fluctuations. The sampling of different configurations will change the vibrational frequency, but if the range of frequencies, Δ, and the time for the fluctuations, τ, satisfy the condition $\Delta\tau < 1$, motional narrowing occurs, and the line shape is Lorentzian. However, as the CLS value is not zero, there is a small degree of inhomogeneity. Careful visual inspection shows that the fresh sample's 2D spectrum is more elongated along the diagonal than that of the annealed sample. For the annealed sample, the CLS value was further reduced to 0.03.

In Figure 5A, we show the CLS versus T_w from the 2D IR spectra of the 2514 cm^{-1} band measured at 298 K. The CLS plots of neither fresh nor annealed gypsum samples show time dependences from T_w = 0.5 to 15 ps. The CLS values fluctuate around the horizontal lines in the figure. Therefore, the inhomogeneous configurations of water do not undergo structural evolution on the time scale of the observations. Again any structural evolution would have to occur on a time scale longer than 1 ns for the lines to appear horizontal over the time range studied. Annealing at 348 K reduced the small degree of quasi-static or static structural disorder significantly, taking the constant CLS value from 0.11 to 0.03. In bulk liquid water, the time scale for complete structural randomization of the hydrogen-bonding network that samples the entire inhomogeneously broadened absorption line is ∼2 ps.[34] Isolated water molecules in the room-temperature ionic liquid, 1-ethyl-3-methylimidazolium bis(trifluoromethylsulfonyl)imide, have several time scales for spectral diffusion. The slowest time scale is ∼20 ps.[37] However, here we find that water molecules confined by the lattice of gypsum do not display picosecond time scale structural evolution, and the structures that give rise to the small amount of inhomogeneous broadening either evolve slowly or are static. This is in contrast to bassanite discussed in the next section.

The total IR absorption line shape is the convolution of the homogeneous Lorentzian line with width Γ and the total inhomogeneous Gaussian line with width Δ_{inh}. The deviation from 1 of the CLS extrapolated to T_w = 0 ps yields the relative

DOI: 10.1021/jacs.6b05589
J. Am. Chem. Soc. 2016, 138, 9694−9703

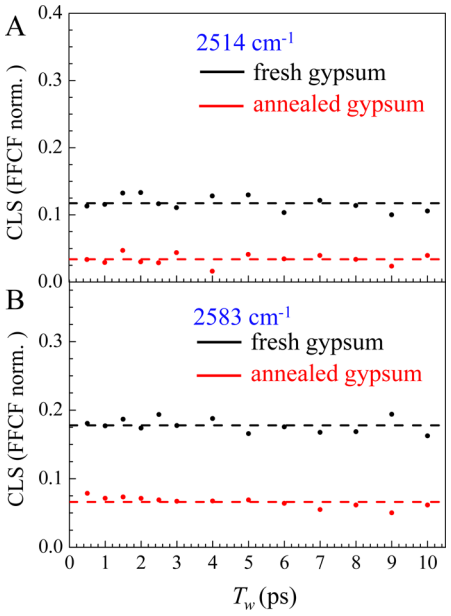

Figure 5. (A) CLS plots versus T_w measured at 2514 cm^{-1} for fresh (black points) and annealed (red points) gypsum samples. The dashed lines are horizontal fits to the data. (B) CLS plot versus T_w measured at 2583 cm^{-1} for fresh (black points) and annealed (red points) gypsum samples. The dashed lines are horizontal fits to the data.

fluctuation amplitude of the homogeneous broadening term in the FFCF. From the FT-IR spectrum, fresh gypsum's full width at half maxima (fwhm) for the 2514 cm^{-1} band is 18.0 cm^{-1}. Based on the CLS and fwhm, we can calculate that Γ = 16.0 cm^{-1} and Δ_{inh} = 2.5 cm^{-1} (see Table 1). Note that Γ is the fwhm of the associated Lorentzian line profile and Δ_{inh} is the standard deviation of the associated Gaussian line profile. After the annealing, Γ increases to 16.8 cm^{-1}, and Δ_{inh} decreases to 1.3 cm^{-1}. The annealed gypsum's total fwhm decreases to 17.4 cm^{-1}, mainly as a result of the decrease in Δ_{inh}. The decrease of Δ_{inh} marks the reduction of inhomogeneity in water configurations.

Eq 7 shows that the OD stretch frequency is very sensitive to O−O distance. As the lattice phonon motions are coupled to the HOD molecule, the O−O distance in the sulfate-water hydrogen bond can fluctuate and sample a range of vibrational frequencies that are motionally narrowed into the homogeneous line. The homogeneous and inhomogeneous line widths as well as the homogeneous dephasing times for all samples are given in Table 1.

In Figure 5B, we show the CLS plots measured for the band at 2583 cm^{-1}. Again, the CLS does not show a time dependence. Similar to the case of 2514 cm^{-1} band, the fresh sample's spectrum is dominated by homogeneous broadening with a small CLS value of 0.18. The total IR absorption line has a fwhm = 15.4 cm^{-1}, where Γ = 12.2 cm^{-1} and Δ_{inh} = 2.9 cm^{-1}. Following annealing, CLS value is reduced to 0.06, and Γ increases by a minor amount to 12.5 cm^{-1}. The total fwhm decreases to 14.0 cm^{-1} as Δ_{inh} decreases to 1.9 cm^{-1}. The reductions in the CLS values of both bands with annealing at the relatively low temperature of 348 K show that annealing significantly reduces the extent of inhomogeneity in the fresh solvent precipitated crystals.

3.2. Bassanite. The FT-IR spectrum of HOD absorption band around 2642 cm^{-1} is presented in Figure 6 (black solid

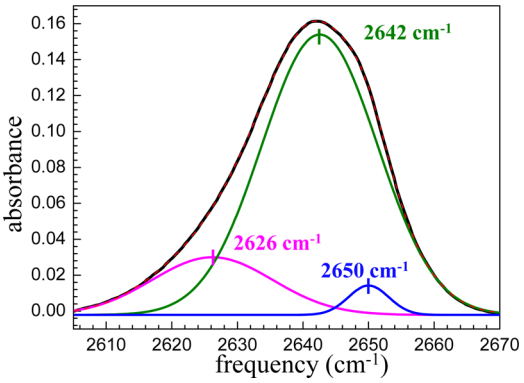

Figure 6. Linear IR absorption spectrum of the OD stretch of HOD in bassanite (16% HOD). The black curve is the measured result. The red dashed curve on top of the black data curve is the fit using three Gaussian components (magenta, dark-green, and blue curves).

curve). The spectrum is asymmetrical with a tail on the red side plus a small shoulder (2650 cm^{-1}) slightly to the blue of the peak center. The experimental line shape can be accurately reproduced with a model of three Gaussian peaks. The dashed red curve is the fit to the total line shape using the three Gaussian model. As is evident from Figure 6, the fit is essentially perfect. The magenta Gaussian component at 2626 cm^{-1} gives rise to the red tail that consists of 16.8% of the total band area. Bassanite's channel structure allows water molecules to be taken up from moisture in air under ambient condition.[5] When the bassanite was exposed to air, the magenta component's relative amplitude versus the other two Gaussians grew significantly while maintaining the same bandwidth and

Table 1. Dynamical Parameters As Measured by 2D IR Spectroscopy

sample[a]	Γ (cm^{-1})[b]	T_2 (ps)	Δ_1 (cm^{-1})	τ_1 (ps)	Δ_2 (cm^{-1})[c]	Δ_{inh} (cm^{-1})	line width (cm^{-1})
gypsum (*f*, 2514 cm^{-1})	16.0	0.66	–	–	2.5	2.5	18.0
gypsum (*a*, 2514 cm^{-1})	16.8	0.63	–	–	1.3	1.3	17.4
gypsum (*f*, 2583 cm^{-1})	12.2	0.87	–	–	2.9	2.9	15.4
gypsum (*a*, 2583 cm^{-1})	12.5	0.85	–	–	1.9	1.9	14.0
bassanite (298 K)	8.2	1.30	4.1	33 ± 2	5.4	6.8	20.7
bassanite (333 K)	10.4	1.02	2.0	11 ± 2	5.4	5.8	19.9
bassanite (348 K)	11.2	0.95	–	–	5.4	5.4	19.6

[a]For gypsum samples, *f* denotes the fresh sample, *a* denotes the annealed sample. [b]Γ refers to the fwhm of the Lorentzian line. Δ_i refers to the standard deviation of the Gaussian line. The total inhomogeneous line width is $\Delta_{inh} = \sqrt{\Delta_1^2 + \Delta_2^2}$. The line width of the entire absorption band is reported in terms of fwhm. [c]Offset term, τ_2 is too long to measure within the experimental time window which is determined by the vibrational lifetime. The Δ_2 for bassanite is determined from data at 348 K which is taken to be the same at 298 and 333 K.

DOI: 10.1021/jacs.6b05589
J. Am. Chem. Soc. 2016, 138, 9694−9703

center position (see Supporting Information). We assign the red wing to HOD molecules residing in channels deformed by additional nonstoichiometric water from moisture. The red-shifted peak position could be caused by a reduced O−O distance between sulfate ions and HOD molecules in defect channels or by additional hydrogen bonds formed between the stoichiometric HOD molecules and the additional H_2O molecules picked up from moisture in the air.

The major component (dark-green curve in Figure 6) is centered at 2642 cm^{-1} with 81.0% of the total band area. This component is assigned to the stoichiometric water in bassanite. From eq 7, the O−O distance of hydrogen bonds between HOD molecules and sulfate ions in bassanite at this frequency is 2.98 Å, which is consistent with analysis based on diffraction measurements.[26] In contrast to gypsum's spectrum, the spectral line is clearly inhomogeneously broadened, as a result of the water molecules in channels populating a range of slightly different configurations.

Oxygen atoms of water molecules in channels coordinate with adjacent calcium ions. The coordinates of water oxygen atoms are stable enough to be observed by X-ray and neutron diffraction studies, though these atoms' Debye−Waller thermal displacement factors are significantly larger than other atoms in the lattice.[25,26] Along the [001] vector, two geometrically distinguishable sites of water oxygen atoms, denoted as O_{w1} and O_{w2}, arrange in a periodic sequence of O_{w1}−O_{w2}−O_{w2} (see Figure 1B). The O−O distance between water sites is ∼5 Å, excluding the possibility of forming hydrogen bonds among these isolated water molecules.[33] For either O_{w1} or O_{w2} site, HOD molecules can form multiple possible sulfate-water hydrogen bonds, with O−O distances at ∼3 Å that match the measured vibrational frequency.[26,33] Water molecules can also dynamically sample different hydrogen-bonding configurations. Therefore, the O_{w1} and O_{w2} water sites are nondistinguishable and both contained within the inhomogeneously broadened Gaussian component at 2642 cm^{-1}.

The small Gaussian component (blue line in Figure 6) at 2650 cm^{-1} is a minor subensemble of HOD molecules, possibly associated with defect sites in the lattice. This minor subensemble is in thermal equilibrium with the major ensemble at 2642 cm^{-1}. As temperature is increased from 298 to 373 K, the major Gaussian barely changes its parameters, while the peak area of the minor subensemble decreases gradually. The change was reversible when the sample was cooled down. Based on temperature-dependent FT-IR spectra, we can estimate that the enthalpy difference of the two ensembles is 12.0 ± 0.2 kJ/mol (see Supporting Information). At an elevated temperature, these HOD molecules can switch to configurations of the major ensemble. Since the minor ensemble's peak area is so small, the conversion of populations between two ensembles barely changes the peak area of the major ensemble. As reported by temperature-dependent X-ray diffraction measurements, there is no significant change in the lattice structure such as phase transitions other than the expansion of cell parameters by ∼0.2% when bassanite is heated over 350 K.[38] Because the structure associated with the subensemble is lower in energy than the main ensemble, the subensemble configurations cannot be accessible to all water molecules, otherwise the 2650 cm^{-1} band would be the major band. Therefore, the subensemble's small population suggests that it is associated with a lattice defect.

Figure 7 shows the anisotropy decays of the OD stretch in bassanite measured at 2644 cm^{-1} (circles). The anisotropy

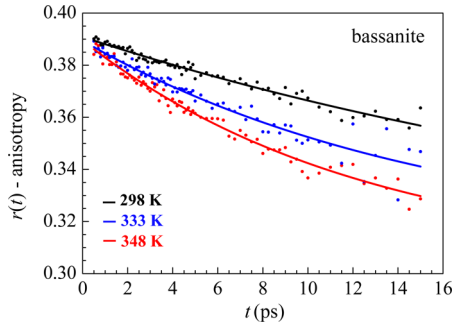

Figure 7. Time-dependent anisotropy decay curves of the OD stretch of HOD in bassanite measured at 298 K (black points), 333 K (blue points), and 348 K (red points). The fits to the data are the solid curves lines.

measured at this frequency corresponds to the dynamics of stoichiometric water sites, as the majority of IR absorption is due to the major Gaussian component in Figure 6. The vibrational population relaxation lifetime is 7.50 ± 0.05 ps. At 298−348 K, the half angle of inertial cone is very small, ∼ 7.5°. This angle is smaller than that observed in gypsum, and indicates that the inertial motion occurs in a more restrictive potential.

Water in bassanite exhibits wobbling-in-a-cone dynamics,[36,39,40] and the decay curves can be fit well with a single exponential term plus an offset term.[40] The OD undergoes orientational diffusion but samples only a limited range of angles on the time scale of the experiments. The decay to a plateau (offset) indicates that complete orientational randomization does not occur or occurs on a time scale much longer than the measurements. The plateau level determines the cone angle. In a crystal, it is likely that the orientation does not undergo complete randomization so long as a water molecule remains in its particular site. Within the fitting error bars, the offset is the same at all temperatures. Therefore, in fitting the data, a single offset was shared for the three curves. The fits are the solid curves in Figure 7.

The diffusive cone half angle is calculated to be 24°. The orientational relaxation time is 29.1 ± 2.5 ps at 298 K. For comparison, the time constant for complete orientational randomization in bulk water is 2.6 ps.[35] At higher temperature, the orientational relaxation time constant decreases gradually: 17.0 ± 1.7 ps at 333 K and 11.9 ± 1.3 ps at 348 K. Based on the temperature-dependent measurements of orientational relaxation time constants, we can calculate that the activation energy for the diffusive wobbling process is 15.2 ± 0.4 kJ/mol. The result corresponds to a scenario where the water oxygen atom positions in channels are moderately confined by weak coordination with calcium ions, while the vectors pointing along the OD bonds can wobble in a small angle restricted by sulfate-water hydrogen bonds.

Figure 8 displays the 2D IR spectra of bassanite measured at 298 K. The top panel is the spectrum at T_w = 0.5 ps. In contrast to the virtually symmetric star-shaped 2D spectra of gypsum, the contour lines in the spectra of bassanite are clearly elongated along the diagonal, demonstrating a significant contribution of inhomogeneous broadening component in the absorption spectrum. As T_w progresses to 15 ps (bottom panel), spectral diffusion causes the shape of 2D spectrum to change. The change in shape between the two spectra is only

DOI: 10.1021/jacs.6b05589
J. Am. Chem. Soc. 2016, 138, 9694−9703

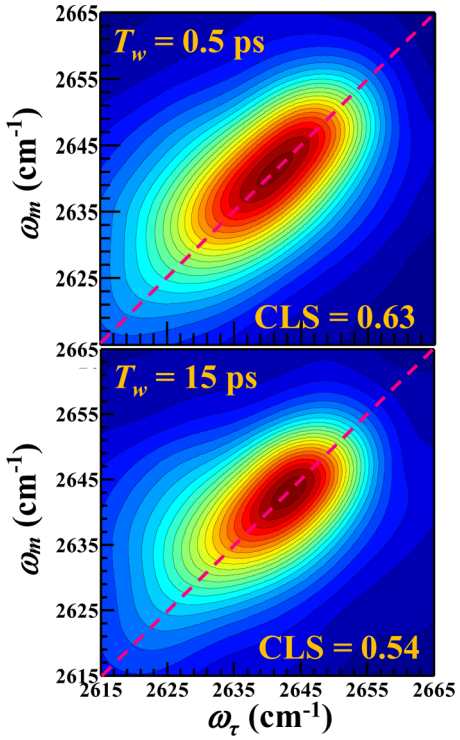

Figure 8. 2D IR spectra of bassanite at 298 K, measured at T_w = 0.5 ps (top panel) and T_w = 15 ps (bottom panel).

moderate, suggesting that the spectral diffusion rate of HOD molecules is relatively slow in bassanite.

The 2D IR spectra of bassanite were measured at three different temperatures: 298, 333, and 348 K. The CLS is calculated around the center of the absorption line where the contributions of the other two low amplitude bands in the spectrum (Figure 6) make negligible contribution to the 2D IR data. In Figure 9 the CLS decays are shown (circles). The initial values of CLS are much higher than that of gypsum but still deviate from 1 by a significant amount. Both homogeneous broadening and inhomogeneous broadening mechanisms are important for the absorption lines of bassanite. At 298 K, the

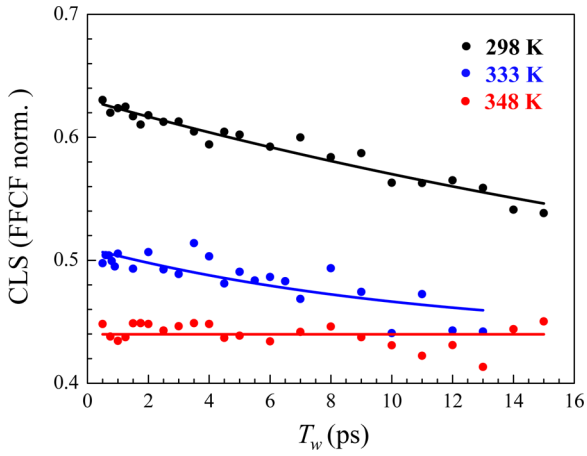

Figure 9. CLS data versus T_w for bassanite at 298 K (black points), 333 K (blue points), and 348 K (red points). The solid lines through the points are the fits. For 398 and 333 K data, the fits are to an exponential with a fixed offset. The red line is the horizontal line through the data points measured at 348 K.

fwhm of the band at 2642 cm^{-1} is 20.7 cm^{-1}. Based on the initial CLS value, we can calculate that Γ = 8.2 cm^{-1} and Δ_{inh} = 6.8 cm^{-1}. Δ_{inh} is the standard deviation, while Γ is the fwhm. The fwhm of the inhomogeneous contribution is 16.0 cm^{-1}. In bassanite, there is a major Gaussian inhomogeneous component, and the absorption has a Voigt line shape as a result of convolution of the Lorentzian and Gaussian components.

Looking at Figure 9, the temperature progression looks strange. At the highest temperature, there is no decay. Only a very slow or static contribution to the CLS is observed. The temperature dependence can be understood in terms of an increase in the homogeneous (motionally narrowed) component of the absorption spectrum as the temperature is raised. The initial CLS value drops as the temperature is increased. At 298 K, the CLS at T_w = 0 has a value of 0.63. This value decreases to 0.51 at 333 K, and further to 0.44 at 348 K. A smaller initial CLS means that the homogeneous component of the absorption line is a larger fraction of the total line width. The physical picture that accounts for the data in Figure 9 is that an increase in temperature speeds up the dynamics. In going from 298 to 348 K, the corresponding homogeneous line widths Γ are 8.2, 10.4, and 11.2 cm^{-1}, and the inhomogeneous line widths Δ_{inh} are 6.8, 5.8, and 5.4 cm^{-1}. When the temperature reaches 348 K, the CLS data no longer display a decay (see Figure 9). The dynamics that gave rise to the decaying components of the CLS at lower temperatures have sped up to the point where all of the components became motionally narrow and become part of the homogeneous line width at 348 K. The result is that at 348 K there are very fast fluctuations that give rise to homogeneous broadening and there is very slowly evolving inhomogeneity or static inhomogeneity that do not produce spectral diffusion within the experimental time window.

First consider the data at 298 K. When the data were fit to a single exponential decay, the result is 103 ± 5 ps. This result assumes that there are no slower or static components of FFCF that fall outside of the experimental time window. 103 ps is the slowest that spectral diffusion could be at 298 K. As discussed above, there is good evidence that there is in fact a very slow or static component in the FFCF of bassanite. Therefore, at room temperature, bassanite undergoes relatively rapid spectral diffusion, but there is also a very slowly evolving or static component to the inhomogeneous broadening. In this model, the inhomogeneous broadening has two components with amplitudes Δ_1 and Δ_2, with Δ_2 being the static component. The total inhomogeneous broadening line width is $\Delta_{inh} = \sqrt{\Delta_1^2 + \Delta_2^2}$.

Because there is no change in the lattice structure of bassanite in the temperature range 298−348 K,[38] we have made the assumption that the amplitude of the quasi-static or static inhomogeneous broadening component of the inhomogeneous line, Δ_2, is temperature independent. Therefore, Δ_2 at lower temperatures is equal to the total inhomogeneous line width at 348 K, which is 5.4 cm^{-1}. Knowing the total inhomogeneous line widths at 298 and 333 K, we can calculate that Δ_1 = 4.1 cm^{-1} at 298 K and Δ_1 = 2.0 cm^{-1} at 333 K. In the normalized FFCF (CLS), the amplitude ratio of the spectral diffusion term and the offset term is $(\Delta_1/\Delta_2)^2$. Now we can confine the fitting model under this condition and fit the CLS decay curve at 298 and 333 K with the model of an exponential term plus a known

DOI: 10.1021/jacs.6b05589
J. Am. Chem. Soc. 2016, 138, 9694−9703

offset term. The spectral diffusion rate was determined to be 33 ± 2 ps at 298 K and 11 ± 2 ps at 333 K.

In going from 298 to 333 K, the decaying component became faster, but its amplitude decreased and the homogeneous line width increased. The increase in temperature sped up the spectral diffusion, and the rate of some of the fluctuations increased to the point that a fraction of the contributions to the inhomogeneous line at lower temperature became motionally narrowed and now contributes to the homogeneous line. The addition to the homogeneous line width was accompanied by a reduction in Δ_1 by 2.1 cm^{-1} from 4.1 to 2.0 cm^{-1}. To have 2.1 cm^{-1} component of the inhomogeneous broadening become motionally narrow, the dynamic fluctuations experienced by the structures that give rise to this portion of the line would have to be faster than ~2.5 ps to make $\Delta\tau < 1$. This fluctuation rate is reasonable.

It is worth noting that in contrast to gypsum, annealing does not occur in bassanite. The temperature-dependent decays shown in Figure 9 are reproducible when the temperature is raised and then lowered. As the OD stretch frequency is sensitive to the sulfate-water O−O distance, the spectral diffusion could correspond to water dynamics that involve the sampling of O−O distance on the time scale of tens of ps.

4. CONCLUDING REMARKS

Recent advances in the methodology of ultrafast nonlinear IR experiments in highly scattering samples made it possible to apply 2D IR and polarization selective pump−probe spectroscopies to investigate the dynamics of water of hydration in minerals, particularly gypsum and bassanite. The samples are granular powders, but it was nonetheless possible to obtain high-quality time-dependent data that provide direct information on water motions inside of these crystals. Both minerals are composed of calcium sulfate but with two waters of hydration per sulfate in gypsum and a half water of hydration per sulfate in bassanite. The difference in the number of water of hydration has a dramatic effect on the water dynamics.

In gypsum, 2D IR measurements show that the water hydroxyl stretch mode has only a very small extent of inhomogeneous broadening prior to annealing of the crystals. The annealed crystals display virtually no inhomogeneous broadening. Static inhomogeneous broadening that can be removed by annealing can be caused by crystal lattice strains. The hydroxyl absorption lines are essentially motionally narrowed homogeneously broadened Lorentzians, which reflect ultrafast motions of the water hydroxyls probably caused by phonons. The pump−probe experiments show that the water molecules do not undergo any diffusive orientational relaxation. There is a small degree of inertial angular motion within a very narrow cone of angles. The ultrafast small degree of angular motion is again most likely caused by coupling of the orientations to phonon-induced motions of the lattice. The results show that water in gypsum is constrained to a single conformation with respect to the lattice and motions of the water occur only on extremely short time scales and most likely occur only because the entire lattice undergoes structural fluctuations caused by phonons that are thermally populated at room temperature.

The behavior of water in bassanite is fundamentally different from gypsum. The water hydroxyl stretch absorption spectrum has substantial inhomogeneous broadening in addition to a homogeneous component as shown by the 2D IR data. Inhomogeneous broadening demonstrates that the water molecules reside in a variety of slightly different configurations with respect to the lattice and in particular with respect to the sulfates to which the hydroxyls are hydrogen bonded. The 2D IR experiments show that at 298 K there is a component of the inhomogeneous broadening that undergoes spectral diffusion on the tens of picoseconds time scale. Spectral diffusion is caused by structural evolution in which the water molecules sample a variety of configurations. As the frequency of the hydroxyl stretch of water that is hydrogen bonded, in this case to sulfate oxygens, is very sensitive to the distance between the water oxygen and the sulfate oxygen, the inhomogeneous broadening and the spectral diffusion are probably caused by the structural evolution that changes the hydrogen bond length.

Analysis of the temperature dependence of the spectral diffusion indicates that there is a component of the inhomogeneity that is static on the time scale of the experimental window, which is determined by the vibrational lifetime of the hydroxyl stretch. As the temperature is increased, the spectral diffusion becomes faster, and an increasing portion of the inhomogeneity becomes motionally narrowed, becoming part of the homogeneous line width rather than the inhomogeneous line width. At the highest temperature studied, 348 K, there is only a homogeneous component and quasi-static or static inhomogeneous component in the absorption line. The inhomogeneity observed at 348 K may randomize on a very slow time scale or it may be caused by strains or defects in the lattice that will remain static on all time scales.

In bassanite, orientational relaxation of the hydroxyl bond is also observed. The orientational motion samples a restricted range of angles, that is, the bond vector wobbles within a cone of angles. As the temperature is increased, the angular sampling becomes faster. Like the 2D IR experiments, the orientational relaxation experiments show that water in bassanite can occupy a restricted range of configurations in the lattice. This configurational freedom, although restricted to a limited range of configurations, is in contrast to gypsum, in which the water molecules are virtually pinned to a single structural configuration in the lattice.

The methods applied here should be applicable to the study of other minerals that have water of hydration as part of their lattice structure. These techniques have previously been applied to the study of metal−organic frameworks, and research using these IR methods is being applied to water in nanoporous silicates.

■ ASSOCIATED CONTENT

Supporting Information

The Supporting Information is available free of charge on the ACS Publications website at DOI: 10.1021/jacs.6b05589.

Comparison of bassanite FT-IR spectra measured at 298 and 348 K, FT-IR spectrum of moisture-affected bassanite, XRD and TGA analysis of gypsum and bassanite samples (PDF)

■ AUTHOR INFORMATION

Corresponding Author

*fayer@stanford.edu

Notes

The authors declare no competing financial interest.

DOI: 10.1021/jacs.6b05589
J. Am. Chem. Soc. 2016, 138, 9694−9703

■ ACKNOWLEDGMENTS

We thank Ming Gong for performing X-ray diffraction measurements. This work was supported by the Air Force Office of Scientific Research grant number FA9550-16-1-0104 (C.Y., J.N., and M.D.F.) and by Division of Chemical Sciences, Geosciences, and Biosciences, Office of Basic Energy Sciences of the U.S. Department of Energy (DOE) grant number DE-FG03-84ER13251 (R.Y. and M.D.F.). C.Y. and J.N. thank the Stanford Graduate Fellowship program for financial support.

■ REFERENCES

(1) Farid, M. M.; Khudhair, A. M.; Razack, S. A. K.; Al-Hallaj, S. *Energ. Convers. Manage.* **2004**, *45*, 1597.
(2) Ojha, L.; Wilhelm, M. B.; Murchie, S. L.; McEwen, A. S.; Wray, J. J.; Hanley, J.; Masse, M.; Chojnacki, M. *Nat. Geosci.* **2015**, *8*, 829.
(3) Laage, D.; Stirnemann, G.; Sterpone, F.; Rey, R.; Hynes, J. T. *Annu. Rev. Phys. Chem.* **2011**, *62*, 395.
(4) Roberts, S. T.; Ramasesha, K.; Tokmakoff, A. *Acc. Chem. Res.* **2009**, *42*, 1239.
(5) Winkler, B. *Phys. Chem. Miner.* **1996**, *23*, 310.
(6) Ferrage, E.; Lanson, B.; Malikova, N.; Plancon, A.; Sakharov, B. A.; Drits, V. A. *Chem. Mater.* **2005**, *17*, 3499.
(7) Sposito, G.; Skipper, N. T.; Sutton, R.; Park, S. H.; Soper, A. K.; Greathouse, J. A. *Proc. Natl. Acad. Sci. U. S. A.* **1999**, *96*, 3358.
(8) Graham, J.; West, G. W.; Walker, G. F. *J. Chem. Phys.* **1964**, *40*, 540.
(9) Madejova, J. *Vib. Spectrosc.* **2003**, *31*, 1.
(10) Sposito, G.; Prost, R. *Chem. Rev.* **1982**, *82*, 553.
(11) Schrodle, S.; Fischer, B.; Helm, H.; Buchner, R. *J. Phys. Chem. A* **2007**, *111*, 2043.
(12) Vandermaarel, J. R. C.; Lankhorst, D.; Debleijser, J.; Leyte, J. C. *J. Phys. Chem.* **1986**, *90*, 1470.
(13) Teixeira, J.; Bellissentfunel, M. C.; Chen, S. H.; Dianoux, A. J. *Phys. Rev. A: At., Mol., Opt. Phys.* **1985**, *31*, 1913.
(14) Ropp, J.; Lawrence, C.; Farrar, T. C.; Skinner, J. L. *J. Am. Chem. Soc.* **2001**, *123*, 8047.
(15) DiCola, D.; Deriu, A.; Sampoli, M.; Torcini, A. *J. Chem. Phys.* **1996**, *104*, 4223.
(16) Pitman, M. C.; van Duin, A. C. T. *J. Am. Chem. Soc.* **2012**, *134*, 3042.
(17) Asbury, J. B.; Steinel, T.; Kwak, K.; Corcelli, S. A.; Lawrence, C. P.; Skinner, J. L.; Fayer, M. D. *J. Chem. Phys.* **2004**, *121*, 12431.
(18) Eaves, J. D.; Loparo, J. J.; Fecko, C. J.; Roberts, S. T.; Tokmakoff, A.; Geissler, P. L. *Proc. Natl. Acad. Sci. U. S. A.* **2005**, *102*, 13019.
(19) Roy, S.; Skoff, D.; Perroni, D. V.; Mondal, J.; Yethiraj, A.; Mahanthappa, M. K.; Zanni, M. T.; Skinner, J. L. *J. Am. Chem. Soc.* **2016**, *138*, 2472.
(20) Piletic, I. R.; Moilanen, D. E.; Levinger, N. E.; Fayer, M. D. *J. Am. Chem. Soc.* **2006**, *128*, 10366.
(21) Merchant, K. A.; Noid, W. G.; Akiyama, R.; Finkelstein, I.; Goun, A.; McClain, B. L.; Loring, R. F.; Fayer, M. D. *J. Am. Chem. Soc.* **2003**, *125*, 13804.
(22) Yan, C.; Yuan, R.; Pfalzgraff, W. C.; Nishida, J.; Wang, L.; Markland, T. E.; Fayer, M. D. *Proc. Natl. Acad. Sci. U. S. A.* **2016**, *113*, 4929.
(23) Nishida, J.; Tamimi, A.; Fei, H. H.; Pullen, S.; Ott, S.; Cohen, S. M.; Fayer, M. D. *Proc. Natl. Acad. Sci. U. S. A.* **2014**, *111*, 18442.
(24) Pedersen, B. F.; Semmingsen, D. *Acta Crystallogr., Sect. B: Struct. Crystallogr. Cryst. Chem.* **1982**, *38*, 1074.
(25) Bezou, C.; Nonat, A.; Mutin, J. C.; Christensen, A. N.; Lehmann, M. S. *J. Solid State Chem.* **1995**, *117*, 165.
(26) Ballirano, P.; Maras, A.; Meloni, S.; Caminiti, R. *Eur. J. Mineral.* **2001**, *13*, 985.
(27) Winkler, B.; Hennion, B. *Phys. Chem. Miner.* **1994**, *21*, 539.
(28) Hamm, P.; Zanni, M. T. *Concepts and Methods of 2D Infrared Spectroscopy*; Cambridge University Press: Cambridge, 2011.
(29) Park, S.; Kwak, K.; Fayer, M. D. *Laser Phys. Lett.* **2007**, *4*, 704.
(30) Kwak, K.; Park, S.; Finkelstein, I. J.; Fayer, M. D. *J. Chem. Phys.* **2007**, *127*, 124503.
(31) Kwak, K.; Rosenfeld, D. E.; Fayer, M. D. *J. Chem. Phys.* **2008**, *128*, 204505.
(32) Seidl, V.; Knop, O.; Falk, M. *Can. J. Chem.* **1969**, *47*, 1361.
(33) Libowitzky, E. *Monatsh. Chem.* **1999**, *130*, 1047.
(34) Park, S.; Moilanen, D. E.; Fayer, M. D. *J. Phys. Chem. B* **2008**, *112*, 5279.
(35) Tan, H.-S.; Piletic, I. R.; Fayer, M. D. *J. Chem. Phys.* **2005**, *122*, 174501.
(36) Szabo, A. *J. Chem. Phys.* **1984**, *81*, 150.
(37) Kramer, P. L.; Giammanco, C. H.; Fayer, M. D. *J. Chem. Phys.* **2015**, *142*, 212408.
(38) Ballirano, P.; Melis, E. *Eur. J. Mineral.* **2009**, *21*, 985.
(39) Wang, C. C.; Pecora, R. *J. Chem. Phys.* **1980**, *72*, 5333.
(40) Tan, H.-S.; Piletic, I. R.; Riter, R. E.; Levinger, N. E.; Fayer, M. D. *Phys. Rev. Lett.* **2005**, *94*, 057405.

DOI: 10.1021/jacs.6b05589
J. Am. Chem. Soc. 2016, 138, 9694−9703